10th CONFERENCE

on

DYNAMICAL SYSTEMS - THEORY AND APPLICATIONS

PROCEEDINGS

Volume 1

EDITORS

J. Awrejcewicz, M. Kaźmierczak, P. Olejnik , J. Mrozowski

Łódź, December 7-10, 2009

POLAND

10th CONFERENCE
on
DYNAMICAL SYSTEMS
THEORY AND APPLICATIONS
December 7-10, 2009. Łódź, Poland

FRACTIONAL DYNAMICS REPRESENTATION IN THE PSEUDO PHASE PLANE

Miguel F. M. Lima, J.A. Tenreiro Machado

Abstract: This paper analyses the spectra of several robotic signals that are approximated by trendlines. The fractional or integer dynamics behavior is determined. For the pseudo phase plane reconstruction of each signal, the time delays are calculated through the fractal dimension, as an alternative to the mutual information that is often used. In order to obtain a smooth pseudo phase plane, the noisy signals are filtered through wavelets. The slopes of the trendlines spectra reveal a relationship with the fractal dimension of the pseudo phase plane and the corresponding time lag.

1. Introduction

The study of fractional order systems received considerable attention recently (Machado 2003), due to the facts that many physical systems are well characterized by fractional models (Podlubny 2002). With the success in the synthesis of real noninteger differentiators, the emergence of new electrical elements (Bohannan 2002), and the design of fractional controllers (Machado 1997; Barbosa *et al.*, 2004), fractional calculus (FC) have been applied in a variety of dynamical processes (Oustaloup *et al.*, 1997). The importance of fractional order mathematical models is that it can be used to make a more accurate description and to give a deeper insight into the physical processes underlying long range memory behaviors. On previous works it was demonstrated that some robotic signals have a fractional behavior and constitute a good test-bed for the study of these phenomena.

A delay differential equation (Driver 1977; Faybishenko 2004; Deng *et al.*, 2007) is a description where the evolution of a system at a certain time, depends on the state of the system at an earlier time. On the other hand, the FC incorporates a memory-time property because it captures the dynamic phenomena involved during all the time-history of a system (Méhauté *et al.*, 1991, Nigmatullin, 2006). Consequently, it seems to exist a relationship between the FC and the integer models with delays, since both are based in memory aspects.

The pseudo phase space (PPS) is used to analyze signals with nonlinear behavior. For the two-dimensional case it is called pseudo phase plane (PPP) (Feeny *et al.*, 2004; Abarbanel *et al.*, 1993; Trendafilova *et al.*, 2001). To reconstruct the PPS it is necessary to find the adequate time lag between the signal and one delayed image of the original signal. To determine the proper time delay often the mutual information concept is used. Nevertheless, in some cases the mutual information reveals a behavior where it becomes difficult to find the adequate time delay. Alternatively, a method based on the fractal dimension to determine the proper delay is proposed in this paper. Some recent research addressed the relationship between fractal dimensions and fractional models (Novikov *et al.*, 2000; Koga *et al.*, 2004; Lima *et al.*, 2008) but, both theoretical and experimental evidences are still to be explored further.

Bearing these ideas in mind, this paper is organized as follows. Section 2 describes the robotic system used to captured the signals. Sections 3 and 4 present some fundamental concepts, and the experimental results, respectively. Finally, section 5 draws the main conclusions and points out future work.

2. Experimental platform

In order to analyze signals that occur in a robotic manipulator an experimental platform was developed. The platform has two main parts: the hardware and the software components. The hardware architecture is shown in figure 1.

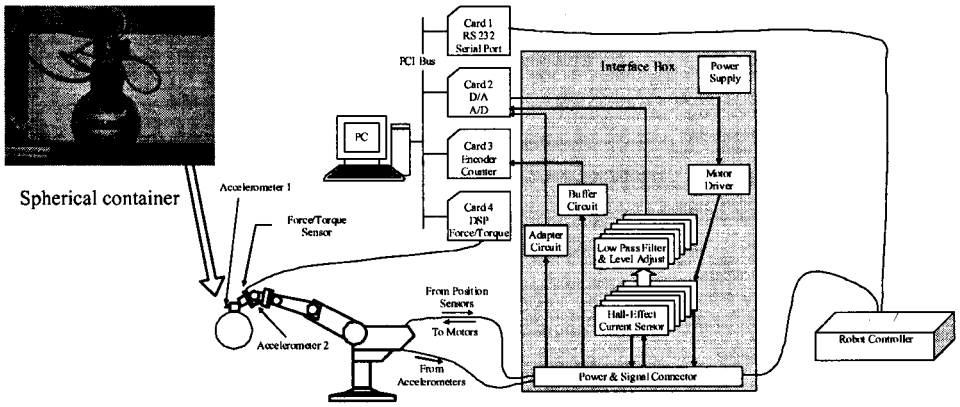

Figure 1. *Hardware architecture.*

Essentially it is made up of a mechanical manipulator, a PC and an interface electronic system. The interface box is inserted between the arm and the robot controller, in order to acquire the internal robot signals. The interface captures also external signals, such as those arising from accelerometers and force/torque sensors. The software package runs in a Pentium 4, 3.0 GHz PC and, from the user's point of view, consists of two applications: (*i*) the acquisition application is a real time program responsible for acquiring and recording the robot signals; (*ii*) the analysis package runs off-line and handles the recorded data. This program includes the Fourier transform (FT), Windowed FT (WFT), correlation, time synchronization, and other signal processing algorithms.

A spherical container carrying a liquid is adopted to test the load dynamics. To analyze the behavior of the variables in different situations, the container (Figure 1) can remain empty or can be filled with a liquid or a solid. The mass of the empty container is 215×10^{-3} kg and its diameter is 203×10^{-3} m. The robot motion is programmed in a way that the container moves from an initial to a final position following a linear trajectory. The signals from different sensors, such as accelerometers, force and torque sensor, position encoders and current sensors are recorded with a sampling period of $t_s = 2 \times 10^{-3}$ s during a total time of $t_T = 20$ s.

3. Main concepts

In this section is presented a review of fundamental concepts involved in the experiments. The technique used to determine the fractional behavior of several robotic signals is based on the slope of their spectra trendlines. Additionally, the PPS is obtained using the method of the time delays. In order to obtain a smooth PPS, the noisy signals captured from the system are filtered using the de-noise capabilities of wavelets.

3.1 Spectrum trendlines

To examine the behavior of the signal FT a trendline is superimposed over the signal spectrum during a bandwidth larger than one decade. The trendline is based on a power law approximation:

$$\left|\mathsf{F}\{f(t)\}\right| \approx c\omega^m \tag{1}$$

where F is the Fourier operator, ω is the frequency, $c \in \Re^+$ is a constant that depends on the signal amplitude, $m \in \Re$ is the slope, f is the signal and t is the time. According to the value of m the signals can exhibit an integer or fractional order behavior.

We must mention that not all signals are possible to approximate through expression (1). In fact, some signals present a scattered spectrum, being difficult to characterize using a simple analytical

expression. Therefore, model (1) is adopted for the signals following approximately that behavior, because it leads to a simple method of comparison.

3.2 Pseudo phase plane and its reconstruction

In the experimental study of the dynamical phenomena usually is not possible to sense all the states in a system. The PPS reconstruction mitigates this lack of information about the system. The goal of the PPS reconstruction is to view the signal in a higher dimensional space taking a sample measurement of its history. In order to achieve the phase space the proper time lag T_d for the delay measurements and the adequate dimension $d \in \mathrm{N}$ of the space must be determined. In the PPP the measurement $s(t)$ forms the *pseudo* vector $y(t)$ according to:

$$y(t) = [s(t), s(t + T_d), \ldots, s(t + (d-1)T_d)] \tag{2}$$

The vector $y(t)$ can be plotted in a d-dimensional space forming a curve in the PPS. There is a one-to-one relationship between the data in the PPS and the associated data in the true state space. If $d = 2$ we have a two-dimensional time delay space. Therefore, the plot of PPP will not change substantially, since the signal $\{s(t), s(t+T_d)\}$ is related with the model $\{s(t), \dot{s}(t)\}$. In resume, we expect the PPP to preserve the major properties of the state space representation, and thus to allow us to draw conclusions about the system dynamics.

The procedure of choosing a sufficiently large d is formally known as embedding, and any dimension that works is called an embedding dimension d_E. The number of measurements d_E should provide a phase space dimension, in which the geometrical structure of the plotted PPS is completely unfold, and where there are no hidden points in the resulting plot.

3.3 Determining the time delays

If we choose T_d too small, then the time series $s(t)$ and $s(t+T_d)$ will be so close to each other (in numerical value) that we cannot distinguish them. From a practical point of view they have not provided us with two independent coordinates. Similarly, if T_d is too large, then $s(t)$ and $s(t+T_d)$ are completely independent of each other (in a statistical sense) and the resulting time series present totally unrelated directions.

Among others (Feeny *et al.*, 2004), the method of delays is the most common method for reconstructing the phase space. Several techniques have been proposed to choose an appropriate time delay (Abarbanel *et al.*, 1993, Choi *et al.*, 1996). Usually the average mutual information (I_{av}) is referred (Feeny *et al.*, 2004; Abarbanel *et al.*, 1993; Trendafilova *et al.*, 2001) as the preferred

alternative to select the proper time delay T_d. It was verified that I_{av} presents a certain degree of noise and oscillation. Consequently, in order to use I_{av} an algorithm must be applied for smoothing the function (Lima *et al.*, 2008). Nevertheless, practice reveals that in some cases is difficult to find the first minimum of I_{av} due to a noise or, even, because it simply does not exist. Due to these issues an alternative is proposed to select the best delay T_d based on the fractal dimension of the PPP.

The fractal dimension is a quantity that gives an indication of how completely a spatial representation appears to fill space. There are many specific methods to compute the fractal dimension. The most popular methods are the Hausdorff dimension and box-counting dimension. Here the box-counting dimension method is used due to its simplicity of implementation and is defined as:

$$\lim_{\varepsilon \to 0} \frac{\ln[N(\varepsilon)]}{\ln(1/\varepsilon)} \tag{3}$$

where $N(\varepsilon)$ represents the minimal number of covering cells (*e. g.*, boxes) of size ε required to cover a set S. The slope on a plot of $\ln[N(\varepsilon)]$ versus $\ln(1/\varepsilon)$ provides an estimate of the fractal dimension.

The tests developed in this article prove that the fractal dimension (*fd*) of the PPP (fd_{PPP}) *versus* the time delay has a maximum corresponding to an adequate value for the chart construction. It should be mentioned that no theoretical proof is provided. The relation between fractal dimension and time delay is only deduced from practical experiments. The same perspective motivates the links between fractal dimension and fractional order, and between fractional dynamics and long memory behavior.

3.4 The Wavelet transform

The continuous wavelet transform (CWT) is a generalization of the WFT. The concept of the WFT consists in multiplying the signal to be analyzed $x(t)$, by a moving window $g(t-\tau)$, and then to compute the Fourier transform of the windowed signal $x(t)\, g(t-\tau)$. Each FT gives a frequency domain 'slice' associated with the time τ at the window centre. Wavelet analysis is performed in a similar way, in the sense that the signal is multiplied by a function called wavelet. However, in the CWT the width of the 'window' changes as the transform is computed. Considering the wavelet function ψ centered at time τ and scaled by s, the CWT of the signal $x(t)$ is represented by:

$$CWT(s,\tau) = \frac{1}{\sqrt{|s|}} \int_{-\infty}^{+\infty} x(t) \psi\left(\frac{t-\tau}{s}\right) dt \tag{4}$$

The CWT of the signal $x(t)$ is a function of two variables: translation τ, that corresponds directly to time, and scale/dilation s, that indirectly relates to frequency information. The transforming function $\psi(t)$ is called mother wavelet, and consists in a prototype for generating the other window functions. The scale s, in the wavelet transform, is similar to the scale used in maps. High scales give a global view of the signal corresponding to the low frequencies in the frequency domain. Low scales give detailed information of a signal corresponding to the high frequencies in the frequency domain,.

The digital version of the CWT is the discrete wavelet transform (DWT) that is considerably faster to implement in a computer. A time-scale representation of a digital signal can also be implemented using digital filtering techniques. An efficient way to implement the DWT using filters was developed by Mallat (Mallat, 1999). Filters of different cutoff frequencies are used to analyze the signal at different scales. The signal is passed through a bank of high pass filters to analyze the high frequencies giving detail information (D_n). Additionally, the signal is passed through a bank of low pass filters to analyze the low frequencies giving a coarse approximation (A_n). Then the decomposition of the signal into different frequency bands is obtained by successive high-pass and low-pass filtering of the time domain signal.

In what concerns to the wavelet function $\psi(t)$ there is a wide variety of wavelet families, that include the Haar, Daubechies, Mexican Hat, Morlet and Meyer wavelets. The function $\psi(t)$ should reflect the type of features present in the time series (Torrence, 1998). Bearing this fact in mind, the wavelet adopted in this paper is a digital version of the Meyer wavelet due to the results obtained and the small computational time.

In this work we use the signal processing capabilities of the DWT for de-noising the experimental signals.

4. Results

According to the platform described in section 2 we adopt an experiment related with the internal movement of the liquid container. Several signals are captured in this experiment and the fractional behavior *versus* the PPP reconstruction is analyzed. All the signals of the trajectories referred previously were studied but, due to space limitations, only the most relevant are depicted.

The signals from the accelerometers and force/moments present a spectrum not well defined in a large frequency range. Therefore, it is difficult to define accurately the behavior of those signals in terms of integer or fractional order (Lima *et al.*, 2008). On the other hand the electrical currents of the axis motors and the position axis seem to be well defined and constitute good candidates for being approximated through trendlines. In this work the behavior of the electrical currents is analyzed for the tree cases, namely container empty, filled with a liquid and filled with a solid.

Figure 3a) shows the amplitude of the FFT of the electrical current of robot axis 5 for the container filled with a liquid. A trendline is calculated and is superimposed over the signal in a frequency range larger than one decade, namely $3 < f < 90$ Hz. The slope of the Fourier spectrum yields $m = -0.96$, revealing, clearly, the integer order behavior. Figure 3b) shows the amplitude of the FFT of the electrical current of robot axis 3 for the empty container case. Again a trendline is calculated, and is superimposed over the spectrum in the same frequency range yielding $m = -1.53$, typical of a fractional order behavior. Figures 3c-d) show the amplitude of the FFT of the electrical current of robot axis 3 for the container filled with a liquid or a solid, respectively yielding $m = -1.48$ for both cases, typical of a fractional order behavior. It is clear that model (1) leads to a simple, but good, approximation.

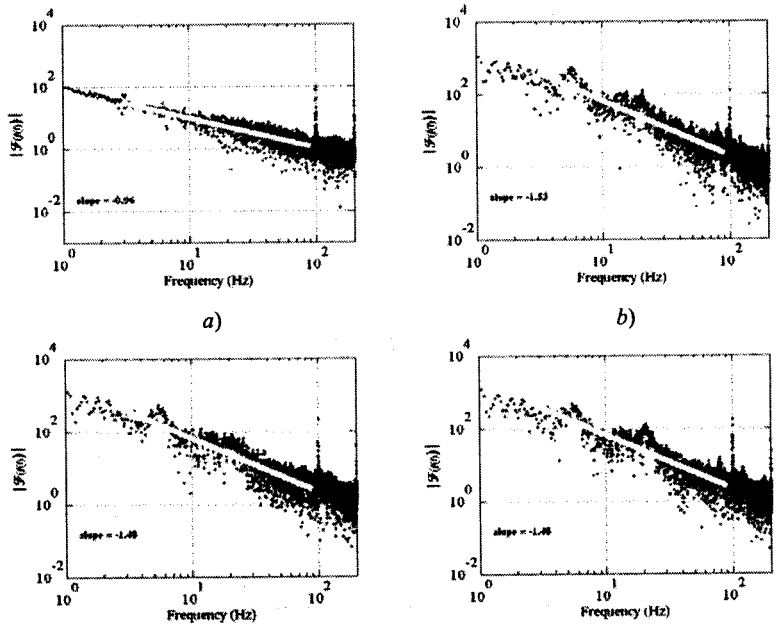

Figure 3. The amplitude of the FFT for the experiment with a liquid container: a) electrical current of robot axis 5 (container filled with a liquid); b) electrical current of robot axis 3 (empty container); c) electrical current of robot axis 3 (container filled with a liquid); d) electrical current of robot axis 3 (container filled with a solid).

According to manufacturer specifications the loop control of the robot has a cycle time of $t_c = 10$ ms. This fact is observed approximately at the fundamental ($f_c = 100$ Hz) and multiple harmonics in all spectra of motor currents.

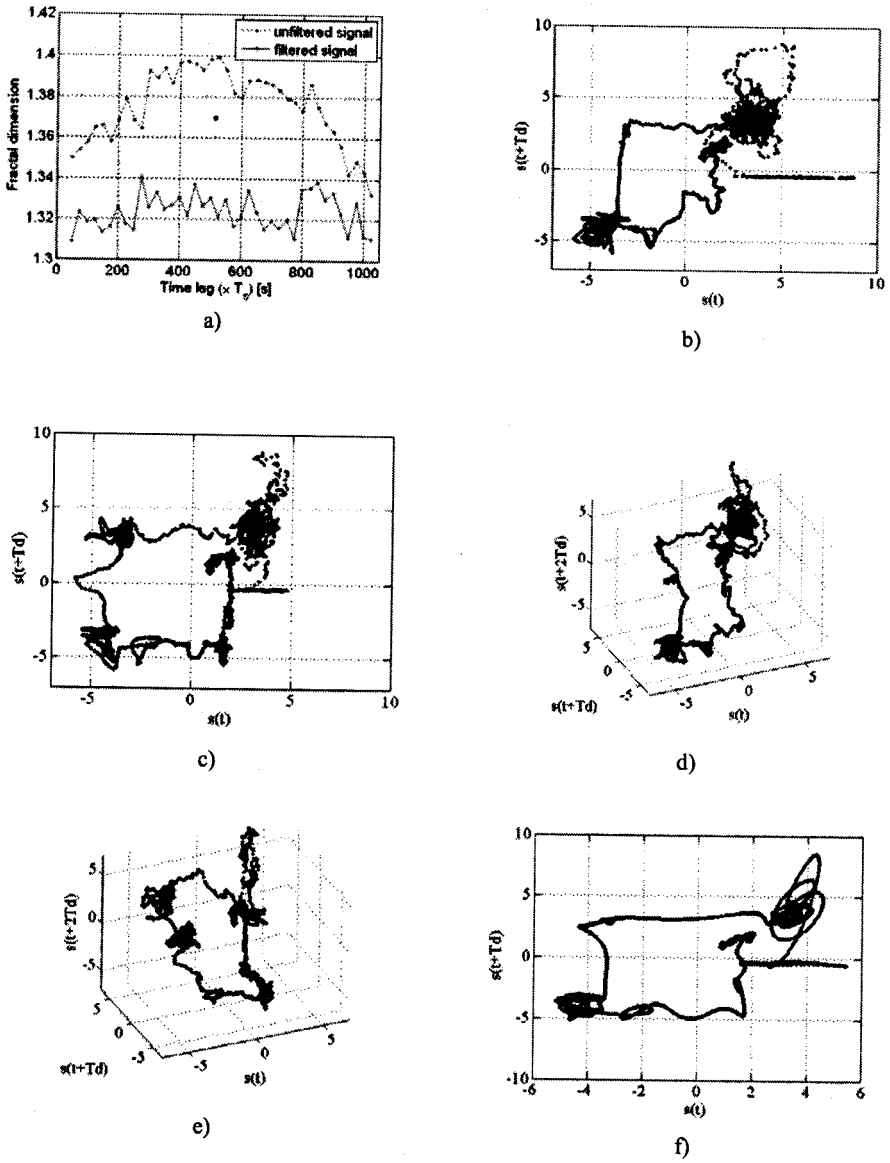

Figure 4. *Indexes of the electrical current of robot axis 3 for the experiment with the liquid container empty: a) fd_{PPP} vs time lag for the original and the filtered signal; b) PPP^{orig} for T_d = 150 samples (0.3s); c) PPP^{orig} for T_d = 525 samples (1.05s); d) 3D PPS^{orig} for T_d = 150 samples; e) 3D PPS^{orig} for T_d = 525 samples; f) PPP^{filt} for T_d = 275 samples (0.55s).*

Figure 4a) depicts *fd versus* the time lag of the electrical current of robot axis 3 for the experiment with the liquid container empty. The fractal dimension of the PPP for the original (fd_{PPP}^{orig}) and for the filtered (fd_{PPP}^{filt}) signals are represented. The step adopted for the time lag calculation was 25 samples (0.05 s) because it represents a useful compromise between the required processing time and the resolution. The index fd_{PPP}^{orig} presents a first local maximum for $T_d = 150$ samples (0.3 s), and a global maximum for $T_d = 525$ samples (1.05 s). In brackets is shown the delay in seconds corresponding to the number of consecutive samples of the time series captured with a sampling frequency of $f_s = 500$ Hz. Figures 4b–c) depict the PPP^{orig} (original not filtered signal) and the PPP^{filt} (filtered signal) for two different time lags of the electrical current of robot axis 3 and the case of the liquid container empty. Several experiments revealed that the adequate PPP is the one corresponding to figure 4c) because it corresponds to the most unfolded chart.

Figures 4d–e) represent the corresponding 3-dimensional PPS where is visible that the unfolded parts of the PPP remains unfolded. Therefore, it seems reasonable to use the fractal dimension of the PPP to gather properties of the PPS. The index fd_{PPP}^{filt} (figure 4a) presents a global maximum for $T_d = 275$ samples (0.55 s) and figure 4f) depicts the corresponding PPP^{filt}. The PPP^{filt} presents a smoother curve when compared with the PPP^{orig}.

Figure 5a) depicts *fd versus* the time lag of the electrical current of robot axis 3 for the experiment with the container filled with a liquid. The fd_{PPP}^{orig} and the fd_{PPP}^{filt} are represented. The corresponding index fd_{PPP}^{orig} presents a global maximum at (T_d, fd_{PPP}^{orig}) = (400, 1.39), although at (T_d, fd_{PPP}^{orig}) = (300, 1.38) the value of fd_{PPP}^{orig} is almost identical. Figures 5b–c) depict the PPP^{orig} for these two different time lags. Practical evaluation reveals that the most adequate PPP is the one corresponding to figure 8c) because it is more unfolded. We can see this feature on $\{s(t), s(t+T_d)\} = \{4, -1\}$. The index fd_{PPP}^{filt} (figure 5a) presents a global maximum for (T_d, fd_{PPP}^{filt}) = (325, 1.301), $T_d = 325$ samples (0.65 s), although at (T_d, fd_{PPP}^{filt}) = (275, 1.300), the value of fd_{PPP}^{filt} is almost identical. Figure 4f) depicts the corresponding PPP^{filt}. The PPP^{filt} presents again a smoother curve when compared with the PPP^{orig}.

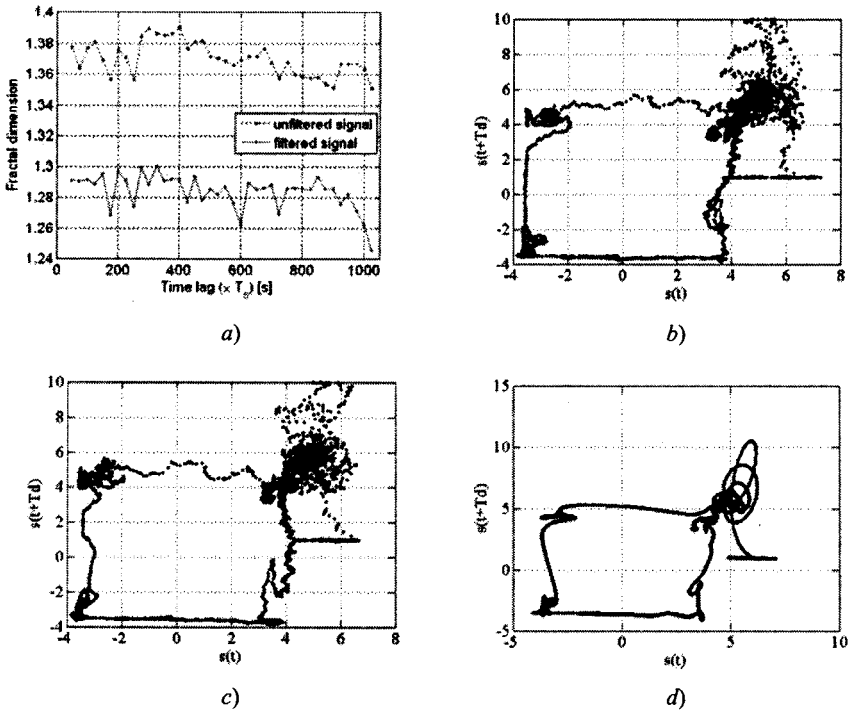

Figure 5. *Indexes of the electrical current of robot axis 3 for the experiment with the container filled with a liquid: a) fd_{PPP} vs time lag for the original and the filtered signal; b) PPP^{orig} for T_d = 300 samples (0.6 s); c) PPP^{orig} for T_d = 400 samples (0.8 s); PPP^{filt} for T_d = 325 samples (0.65s).*

Figure 6a) depicts the fd_{PPP}^{orig} and the fd_{PPP}^{filt} *versus* the time lag of the electrical current of robot axis 3 for the experiment with the container filled with a solid. The corresponding index fd_{PPP}^{orig} presents a global maximum for T_d = 300 samples (0.6 s). Figures 6b) depicts the corresponding PPP^{orig}. The index fd_{PPP}^{filt} (figure 6a) presents a global maximum for T_d = 275 samples (0.55 s). Figure 6c) depicts the corresponding PPP^{filt}. Again, the PPP^{filt} presents a smoother behavior when compared with the PPP^{orig}.

The PPP charts shown previously have a kind of 'clouds' particularly at the corners. These clouds can hide superimposed curves. To unfold the curves we must find the proper embedding dimension. A key property of the embedding is that the mapping from the real space to the pseudo space is one-to-one. If trajectories cross each other in the PPP, then it is not an embedding (Feeny *et al.*, 2004). A deeper insight into the nature of this feature must be envisaged to understand the behavior of the PPP.

After analyzing individually the behavior of some electrical currents we will explore some relationship between the variables. Figure 7 depicts the trendline slopes *versus* fd_{PPP} and T_d for the electrical current of all robot axis motors for the three cases of the container: empty, filled with a solid and filled with a liquid. Those fifteen points leads to the surfaces shown in figure 7 and the relationship between the three variables. Figure 7a) presents the surface obtained for the unfiltered signals, while figure 7b) presents the surface obtained for the filtered signals with wavelets.

We observe a smooth curve linking the trendline slopes *versus* fd_{PPP} and T_d, establishing a relationship between the three variables.

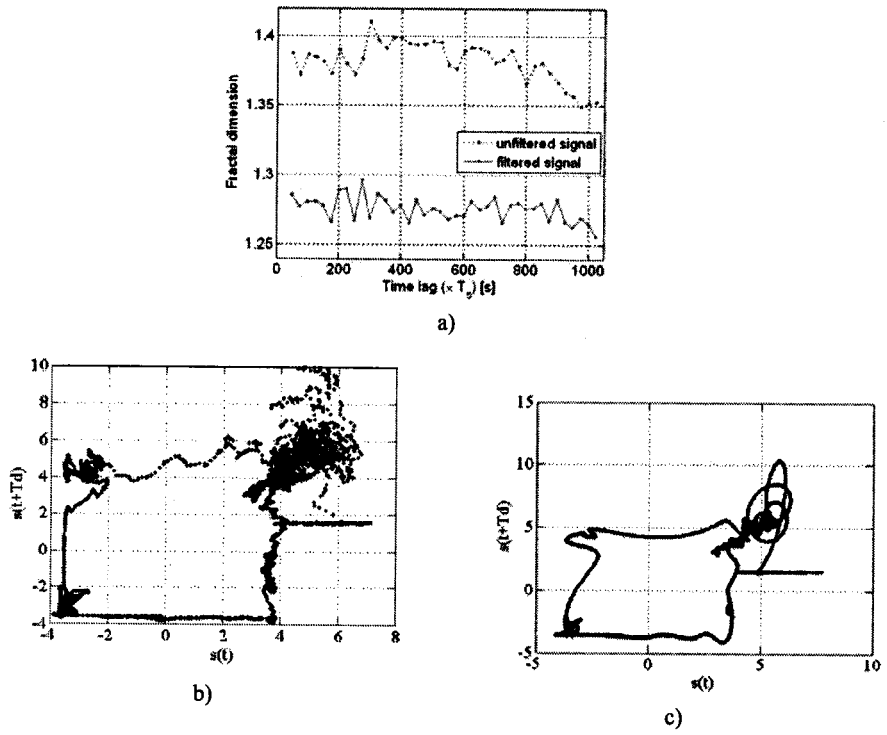

Figure 6. *Indices of the electrical current of robot axis 3 for the experiment with the container filled with a solid: a) fd_{PPP} vs time lag for the original and the filtered signal; b) PPP^{orig} for T_d = 300 samples (0.6 s); c) PPP^{filt} for T_d = 275 samples (0.55s).*

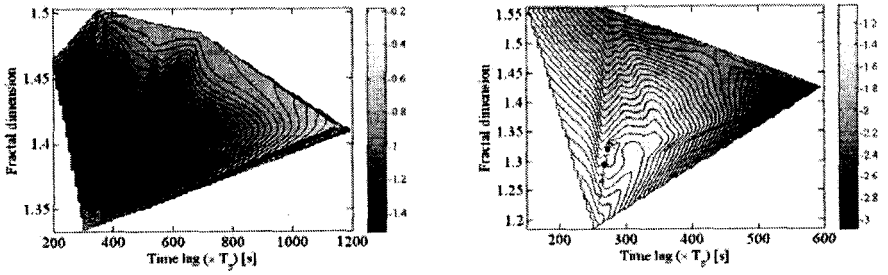

a) *b)*

Figure 7. *Trendline slopes of the electrical motor currents spectra vs fd_{PPP} and time lag for the three cases of the container, empty, filled with a solid and filled with a liquid: a) unfiltered signals; b) filtered signals*

5. Conclusions

The spectrum of several robotic signals was approximated by trendlines. Based on the slope of the trendlines the fractional or integer order behavior was determined. For the PPP reconstruction of each signal an approach based on the fractal dimension was used to find the appropriate time lag. To obtain a smooth PPP the noisy signals captured from the system are filtered through wavelets.

After analyzing individually the behavior of the electrical motor currents of a robotic system, were plotted the trendline slopes *versus* fd_{PPP} and the time lagged, for the container empty, filled with a solid and filled with a liquid. The plots reveal that all the points are located in a locus that demonstrate a relationship between the variables, both for the noisy and the filtered signals.

References

Abarbanel, H. D. I., Brown, R., Sidorowich, J. J., Tsimring, L. Sh., "The analysis of observed chaotic data in physical systems", *Reviews of Modern Physics*, vol. 65, n. 4, p. 1331-1392, 1993.

Barbosa, Ramiro S., J. A. Tenreiro Machado, Isabel M Ferreira, "Tuning of PID Controllers Based on Bode's Ideal Transfer Function", *Nonlinear Dynamics*, 38: pp. 305–321, Kluwer Academic Publishers, 2004.

Bohannan, Gary W. "Analog Realization of a Fractional Control Element –Revisited" mechatronics.ece.usu.edu/foc/cdc02tw/cdrom/aditional/FOC_Proposal_Bohannan.pdf, 2002.

Choi, Jae-Gyun, Jong-Keun Park, Kwang-Ho Kim, Jae-Cheol Kim, "A daily peak load forecasting system using a chaotic time series", *Proc. Int. Conf. on Intelligent Systems Applications to Power Systems*, IEEE; 28 Jan–2 Feb 1996 Page(s):283 – 287 doi:10.1109/ISAP.1996.501083.

Deng, W. H., C. P. Li, J. Lü, "Stability analysis of linear fractional differential system with multiple time-delays", *Nonlinear Dynamics*, 2007, 48(4): 409-416.

Driver, Rodney. D., *Ordinary and Delay Differential Equations*, Applied Mathematical Sciences 20, Springer-Verlag NY, 1977, ISBN 0-387-90231-7.

Faybishenko, B. (2004), "Nonlinear dynamics in flow through unsaturated fractured porous media: Status and perspectives", *Rev. Geophys.*, 42, RG2003, doi:10.1029/2003RG000125.

Feeny, B. F., G. Lin, "Fractional derivatives applied to phase-space reconstructions," *Nonlinear Dynamics*, 38 (1-4) 85-99, 2004, special issue on fractional calculus.

Koga, Hiroyuki, Masahiro Nakagawa, "Method of evaluation of fractal dimensions in terms of fractional integro-differential equations", *Electronics and Communications in Japan* (Part III: Fundamental Electronic Science), vol. 87, n. 4 , p.p. 30–39, 2004.

Lima, Miguel F. M., J.A. Tenreiro Machado, Manuel Crisóstomo, Fractional Dynamics in Mechanical Manipulation, Journal of Computational and Nonlinear Dynamics, Transactions of the ASME, Vol. 3, Issue 2, April 2008, available online 4 Feb. 2008, pp. 021203-1 – 021203-9, doi: 10.1115/1.2833488, ISSN 1555-1423.

Lima, Miguel F. M., J.A. Tenreiro Machado, Manuel Crisóstomo, "Pseudo Phase Plane, Delay and Fractional Dynamics in Robotic Signals", JESA – Journal Européen des Systèmes Automatisés, special issue on fractional differentiation, Hermes, vol. 42, n° 6-7-8, Aug-Out/2008, pp. 1037-1051, ISBN-978-2-7462-2262-5.

Machado, J. A. Tenreiro, "Analysis and Design of Fractional-Order Digital Control Systems", *Journal Systems Analysis-Modelling-Simulation*, Gordon & Breach Science Publishers, vol. 27, pp. 107-122, 1997.

Machado, J. A. Tenreiro, "A Probabilistic Interpretation of the Fractional-Order Differentiation", *Journal of Fractional Calculus & Applied Analysis*, vol. 6, No 1, pp. 73-80, 2003.

Mallat S., "A Wavelet Tour of Signal Processing", Academic Press, 1999.

Méhauté, Alain Le, Jack Howlett, *Fractal geometries: theory and applications*, CRC Press, Inc., Boca Raton, FL, 1991.

Nigmatullin, R.R., "'Fractional' kinetic equations and 'universal' decoupling of a memory function in mesoscale region", *Physica A: Statistical Mechanics and its Applications*, volume 363, Issue 2, 1 May 2006, Pages 282-298, doi:10.1016/j.physa.2005.08.033.

Novikov, V. V., K. V. Voitsekhovskii, "Viscoelastic properties of fractal media", *Journal of applied mechanics and technical*, vol. 41, n. 1, pp. 149–158, 2000.

Oustaloup, Alain, Xavier Moreau, Michel Nouillant, "From fractal robustness to non integer approach in vibration insulation: the CRONE suspension", *Proceedings of the 36th Conference on Decision & Control*, San Diego, California, USA, December, 1997.

Podlubny, I., "Geometrical and physical interpretation of fractional integration and fractional differentiation", *Journal of Fractional Calculus & Applied Analysis*, vol. 5, No 4, pp. 357-366, 2002.

Torrence, C. and G. P., Compo., "A Practical Guide to Wavelet Analysis." Bulletin of the American Meteorological Society. 1, 1998, Vol. 79, pp. 61-78.

Trendafilova, I., H. Van Brussel, "Non-linear dynamics tools for the motion analysis and condition monitoring of robot joints", *Mech. Sys. and Signal Proc.*, vol.15, issue 6, pp. 1141–1164, Nov 2001, available online 2 Oct 2007, doi:10.1006/mssp.2000.1394.

Miguel F. M. Lima.
Dept. of Electrical Engineering Superior School of Technology
Polytechnic Institute of Viseu
3504-510 Viseu, Portugal
lima@mail.estv.ipv.pt

J. A. Tenreiro Machado.
Dept. of Electrical Engineering
Institute of Engineering
Polytechnic Institute of Porto
4200-072 Porto, Portugal
jtm@isep.ipp.pt